



# Morphological and molecular characterization of a new freshwater microsporidium, *Jirovecia sinensis* sp. n. (Microsporidia) infecting the coelomocytes of *Branchiura sowerbyi* (Oligochaeta: Naididae) in China



Xinhua Liu<sup>a,b</sup>, Meiqi Wen<sup>b,d</sup>, Yuanli Zhao<sup>b,d</sup>, Aihua Li<sup>b,d</sup>, Jinyong Zhang<sup>b,c,d,\*</sup>

<sup>a</sup> Laboratory of Hydrobiology, Hunan Agricultural University, Changsha 410128, China

<sup>b</sup> Key Laboratory of Aquaculture Diseases Control, Ministry of Agriculture, State Key Laboratory of Freshwater Ecology and Biotechnology, Institute of Hydrobiology, Chinese Academy of Sciences, Wuhan 430072, China

<sup>c</sup> School of Marine Science and Engineering, Qingdao Agricultural University, Qingdao, Shandong Province 266109, China

<sup>d</sup> University of Chinese Academy of Sciences, Beijing 100049, China

## ARTICLE INFO

### Keywords:

Microsporidia

Oligochaete

*Jirovecia sinensis* sp. n.

SSU rDNA

Electron microscopy

## ABSTRACT

We report a new microsporidium *Jirovecia sinensis* sp. n. from a freshwater oligochaete, *Branchiura sowerbyi* collected in Hongze city, Jiangsu province, East China. Numerous whitish hypertrophied coelomocytes of 0.33–0.59 mm in diameter indicated infection. Transmission electron microscopy observations revealed that all developmental stages were diplokaryotic. The earliest life stages observed were meronts that were in direct contact with host cytoplasm, accumulated peripherally in the hypertrophied coelomocytes and connected with host cytoplasm through many pinocytotic canals. Mature spores are rod-shaped with a blunt end, measuring  $17.0 \pm 0.1$  (14.9–18.5)  $\mu\text{m}$  long and  $2.0 \pm 0.2$  (1.7–2.2)  $\mu\text{m}$  wide. The most conspicuous character of the novel microsporidian parasite is the tail-like posterior prolongations, with a length of 29.6–40.8  $\mu\text{m}$ . Mature spores have a manubrium with a diameter of 447–485 nm which consist of six density-discontinuous concentric circles. Spores possess a collar-shaped anchoring disk and a bipartite polaroplast with an anterior lamellar region and a posterior tubular section. SSU rDNA-based phylogenetic analysis indicated with high support values that the new species clustered with two *Bacillidium* species (*B. vesiculoformis* and *Bacillidium* sp.) infecting the freshwater oligochaetes and *Janacekia debaisieuxi* infecting the insect *Simulium maculatum*. Based on the ultrastructural features and molecular characteristics, a new species in the genus *Jirovecia*, *Jirovecia sinensis* sp. n., is designated.

## 1. Introduction

Microsporidia are obligate intracellular parasites that are widely suggested to be related to Fungi (Corradi and Keeling, 2009; Vossbrinck et al., 2014). Microsporidia possess a unique invasion organelle, the polar tube, which rapidly discharges out of the spores, and injects the sporoplasm into the host cytoplasm upon appropriate environmental stimulation (Han and Weiss, 2017; Stentiford et al., 2013; Vávra and Larsson, 2014). Since the first microsporidium, *Nosema bombycis*, was reported in 1857, about 1600 species assigning to more than 200 genera had been reported worldwide (Franzen, 2008; Stentiford et al., 2013). Among them, around half were discovered from aquatic organisms including fishes, aquatic arthropods and non-arthropod

invertebrates and protists. Aquatic microsporidia reported in China were mainly from fishes and cultured shrimps and crabs, however, no species were reported from other invertebrates, such as oligochaetes, an important host group of Microsporidia (Xu et al., 2017; Wang et al., 2017).

*Jirovecia* species primarily infect freshwater oligochaetes with the exception of *Jirovecia brevicauda*, which invades the fat body of *Chironomus riparius* (Insecta: Diptera) larvae (Larsson, 1986, 1989, 1990a). Species of *Jirovecia* are typically characterized by a large rod-shaped spore with a tail-like posterior prolongation. The polar filament of *Jirovecia* spp. possess an anterior manubrium which is unusual for most aquatic microsporidia. Currently, an integrative taxonomic approach of considering spore morphology, ultrastructural features of all

\* Corresponding author at: Key Laboratory of Aquaculture Diseases Control, Ministry of Agriculture, State Key Laboratory of Freshwater Ecology and Biotechnology, Institute of Hydrobiology, Chinese Academy of Sciences, Wuhan 430072, China. School of Marine Science and Engineering, Qingdao Agricultural University, Qingdao, Shandong Province 266109, China.

E-mail address: [zhangjy@ihb.ac.cn](mailto:zhangjy@ihb.ac.cn) (J. Zhang).

developmental process and molecular data (mainly SSU rDNA sequence) is widely accepted and recommended to identify microsporidia (Andreadis et al., 2018; Stentiford et al., 2013; Vossbrinck and Debrunner-Vossbrinck 2005). All six reported *Jirovecia* species, however, were described in the 20th Century based solely on ultrastructural characteristics (Larsson, 1986, 1989, 1990a; Larsson and Götz, 1996) and no molecular data are available. For the first time, molecular characterization of a representative *Jirovecia* species has been conducted, which provides the position of this genus on the Microsporidia SSU rDNA-based phylogenetic tree. Here, we described a novel species, *Jirovecia sinensis* sp. n., infecting the coelomocytes of *Branchiura sowerbyi*.

## 2. Material and methods

### 2.1. Sample collection and light microscopy observation

A total of 682 oligochaete specimens, ranging from 13.3 cm to 18.5 cm in length, were collected from a pond of cultured gibel carp, *Carassius auratus gibelio* (Bloch) in Hongze city, Jiangsu province, East China (33°21'20"N, 118°52'47"E). All live samples were transported to the local diseases laboratory of aquatic animals for parasitological examination using observation, stereomicroscopy and light microscopy. Macroscopic whitish xenoma-like formations in *B. sowerbyi* were easily observed. Wet mounts of the xenoma-like formations were examined under light microscopy (Motic BA210; Motic, China) and photographed using Olympus BX 53 microscope equipped with an Olympus DP72 digital camera (Olympus, Japan). The remaining xenoma-like formations were preserved in 95% ethanol and 2.5% glutaraldehyde in 0.1 M sodium cacodylate buffer (PH 7.4) for molecular analyses and transmission electron microscopic (TEM) observations, respectively.

### 2.2. Transmission electron microscopy

Approximately 1 week after fixation, samples were transferred to a fresh portion of the same fixative for 1 h, washed with sodium cacodylate buffer twice (10 min) and placed into 1% Osmium tetroxide (OsO<sub>4</sub>) solution for 1 h. After dehydration through a gradual ascending series of ethanol and propylene oxide series, the samples were embedded in Spur resin. Ultrathin sections (70–90 nm) of target areas were mounted on uncoated copper grids and stained with uranyl acetate and lead citrate. Grids were examined using a Hitachi HT-7700 transmission electron microscope.

### 2.3. DNA extraction, PCR and sequencing

In order to remove ethanol remnants, preserved xenoma-like formations isolated from the infected *B. sowerbyi* were centrifuged and washed twice with distilled water. The isolated xenoma-like formations were homogenized using Lysing Matrix B FastPrep® tubes and a Fast Perp cell disrupter (1 min at 6 m s<sup>-1</sup>). Genomic DNA was extracted from the homogenate using a commercial tissue extraction kit (Qiagen, Hilden, Germany) and following the manufacturer's instructions for animal tissue. For the amplification of SSU rRNA gene, the microsporidian-specific primer pairs v1f (5'-CACCAAGGTTGATTCTGCCT GAC-3') and 1492r (5'-GGTTACCTTGTACGACTT-3') were used (Nilzen, 2000; Vossbrinck and Debrunner-Vossbrinck, 2005). PCR reactions were conducted in a 50-μl reaction mixture containing PCR buffer, 200 mM dNTP, 2 mM MgCl<sub>2</sub>, 1.25 units Taq polymerase, 20 pm each primer and 2 μl DNA template. Thermocycler parameters were as follows: an initial denaturation step at 95 °C for 4 min, followed by 35 cycles of denaturation at 94 °C for 1 min, annealing at 46 °C for 30 s, elongation at 72 °C for 2 min and a final extension at 72 °C for 10 min. The target PCR products were excised from an agarose gel and purified using a PCR purification kit (CWBiotech, Beijing, China) and cloned into a PMD-18 T vector system (Takara, Tokyo, Japan). Positive clones

were randomly selected and sequenced in both directions with the ABI BigDye Terminator v3.1 Cycle Sequencing Kit with an ABI 3100 Genetic Analyzer.

### 2.4. Molecular analysis

Sequences were assembled by BioEdit (Hall, 1999). The consensus sequences were deposited in GenBank with accession numbers MN752317 and MN752318 and verified as a microsporidium by BLAST search. Sequences with high similarity and others of interest were retrieved from the GenBank database. A total of 40 sequences were aligned with Clustal X by default setting (Thompson et al., 1997). The alignment was corrected manually using alignment editor of the software MEGA 6.0 (Tamura et al., 2013). Phylogenetic reconstructions were conducted using the maximum likelihood (ML) method in PhyML 3.0 and Bayesian inference (BI) in Mr. Bayes (Guindon et al., 2010; Ronquist and Huelsenbeck, 2003). The optimal evolutionary model for ML and BI was determined to be GTR + I + G by jModelTest 3.07 (Posada, 2008) using the Akaike information criteria. Two independent runs were conducted with four chains for 1 million generations for BI. Phylogenetic trees were sampled every 100 generations. The first 25% of the samples were discarded from the cold chain (burninfrac = 0.25). Bootstrap confidence values were calculated with 100 replicates for ML. Trees were initially examined in Figtree v1.4.4 (<http://tree.bio.ed.ac.uk/software/figtree/>), edited and then annotated in Adobe Illustrator (Adobe System, San Jose, CA, USA).

## 3. Results

### 3.1. Macroscopic observations and light microscopy

During the survey of the diversity of microsporidia in freshwater oligochaetes in China, three oligochaete species, *Limnodrilus hoffmeisteri*, *L. claparedeianus* and *Branchiura sowerbyi* were examined. Oligochaete specimens were morphologically identified with assistance of taxonomists for aquatic zoobenthos, Dr. Cui and Prof. Wang in Institute of Hydrobiology, Chinese Academy of Sciences. Among them, 50 *B. sowerbyi* were found to be infected, with microsporidia in the coelomocytes (Fig. 1A), and with a prevalence of 11.0% (50/456). The infected hypertrophied coelomocytes presented as easily observed whitish xenoma-like formations (Fig. 1A). After puncturing the integument of oligochaetes, numerous xenoma-like formations filled with rod-shaped spores were released (Fig. 1A–C). Although bearing a high burden of xenoma-like formations along most of the body, the infected oligochaetes appeared to move as normally as uninfected individuals (Unpublished results). The whitish xenoma-like formations were ellipsoidal and measured 0.33–0.59 mm in diameter. Mature spores were rod-shaped with a long tail-like posterior prolongation, a typical feature of the *Jirovecia* genus, and measured 17.0 ± 0.1 (14.9–18.5) μm long and 2.0 ± 0.2 (1.7–2.2) μm wide (N = 30) (Fig. 1B, C).

### 3.2. Ultrastructural observations

Transmission electron microscopy showed numerous developmental stages of the microsporidium in the hypertrophied coelomocytes (Figs. 2 and 3). Development was asynchronous; meronts, sporoblasts and mature spores could be observed in an individual infected hypertrophied coelomocyte (Fig. 2A). All life stages contained diplokaryotic nuclei. Within the hypertrophied coelomocytes, masses of presporogonic stages accumulated peripherally, whereas mature spores were located centrally (Fig. 2A). Numerous pinocytotic canals located peripherally in the hypertrophied coelomocytes were presumed to be involved in nutrient uptake from the host cytoplasm (Fig. 2A, B). The earliest developmental stages observed were late meronts and variable electron dense substances, ribosomes and endoplasmic reticulum materials filled the cells (Fig. 2C, D). The meronts, residing in direct

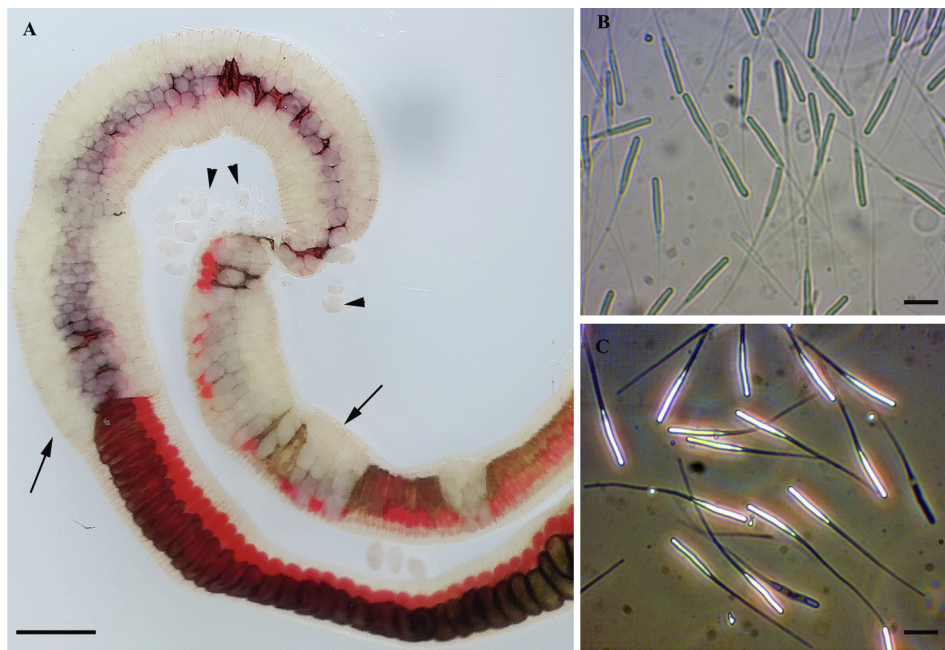


**Fig. 1.** Light microscopy of *Jirovecia sinensis* sp. n. infecting the coelomocytes of *Branchiura soweryi*. A. Clinical signs of microsporidiosis in *Branchiura soweryi* included numerous whitish xenoma-like formations, scale bar = 0.2 cm; B. Fresh spores observed under light microscopy; C. Phase-contrast image of fresh spores. Scale bar: B, C, 10  $\mu$ m.

contact with host cell cytoplasm, were diplokaryotic with a notably large oval diplokaryon measuring 3.5–3.8  $\mu$ m in diameter occupying most of the cell volume (Fig. 2C, D). The diplokaryotic nuclei of meront were of the same size; nuclei that were unequal in size were rarely observed and were possibly due to irregular cuts (Fig. 2C, D). Sporonts were not detected and the number of sporoblasts per sporont was unknown. Early sporoblasts were of irregular shape and were in direct contact with host cytoplasm (Fig. 2E). Sporoblasts developed into spores by elongation of the parasite cells accompanied by the

development of the structures typical for mature spores, including the manubrium, trilaminar spore wall and tail-like projection on the posterior end of the spores. The cell wall of the sporoblast was 83.3–112.5 nm thick and consisted of the electron dense exospore 28.1–40.6 nm thick, electron lucent endospore 53.1–65.5 nm thick and thin, 8 nm, plasma membrane (Figs. 2F, 3A, G).

Mature spores were diplokaryotic and rod-shaped with a long tail-like posterior prolongation (extension of exospore material) with length 29.6–40.8  $\mu$ m (Fig. 3D, E). Each spore was generally enclosed within a

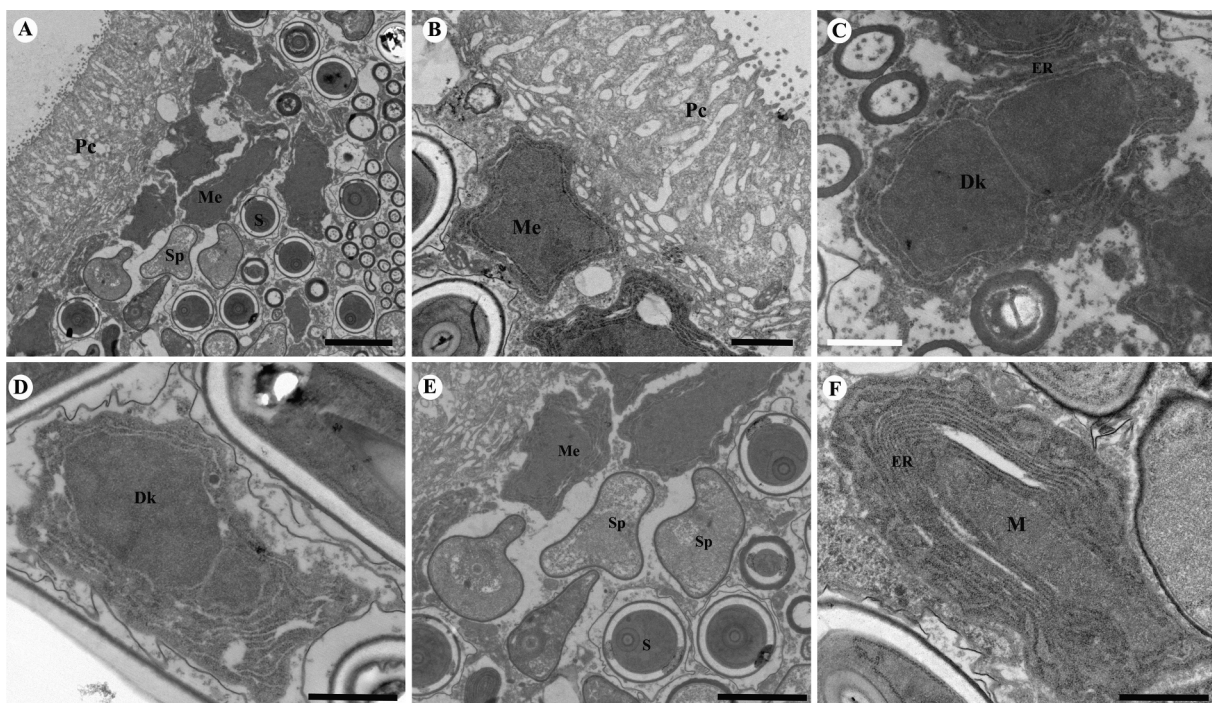


**Fig. 2.** Electron micrographs of *Jirovecia sinensis* sp. n. spores. A. Ultrastructure of the periphery of xenoma-like formations showing meronts (Me), sporoblasts (Sp), mature spores (S) and pinocytotic canals (Pc), scale bar = 3  $\mu$ m; B. Magnification of the ultrastructure of the periphery of xenoma-like formations showing meronts (Me) and pinocytotic canals (Pc), scale bar = 1  $\mu$ m; C. Late meront with diplokaryotic nucleus surrounded by numerous endoplasmic reticula (ER), scale bar = 1  $\mu$ m; D. A meront with unequal diplokaryotic nucleus, scale bar = 2  $\mu$ m; E. Different developmental stages accumulated in the periphery of xenoma-like formations, scale bar = 2  $\mu$ m; F. The anterior region of a sporoblast exhibiting the ultrastructure of manubrium (M) and endoplasmic reticulum (ER), scale bar = 1  $\mu$ m.

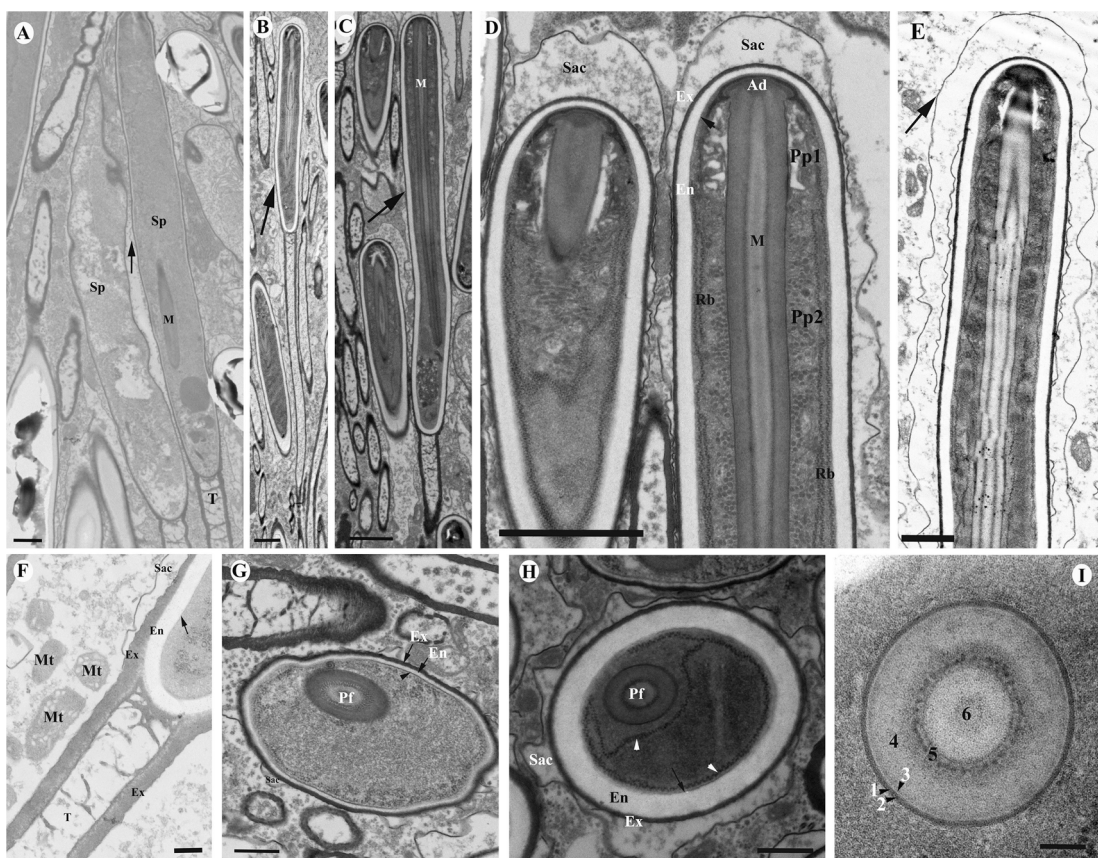


**Fig. 3.** Electron micrographs of spores of *Jirovecia sinensis* sp. n. A. Sac (arrow), manubrium (M), trilaminar spore wall and tail-like posterior prolongation (T) appearing in sporoblasts stages (Sp), scale bar = 1  $\mu$ m; B. A mature spore with tail-like posterior prolongation (arrow), scale bar = 2  $\mu$ m; C. A mature spore (arrow) showing the manubrium occupying three-quarters of spore body length, scale bar = 2  $\mu$ m; D. The magnification of anterior region of spores showing the ultrastructure of sac, anchoring disk (Ad), manubrium (M), the lamellar polarplast (Pp1) and tubular polarplast (Pp2), ribosomes (Rb) and the trilaminar spore wall including exospore (Ex), endospore (En) and plasma membrane (arrow), scale bar = 2  $\mu$ m; E. A spore enclosing within two sacs (arrow), scale bar = 1  $\mu$ m; F. Magnification of the posterior of spore showing the ultrastructure of tail-like prolongation, scale bar = 500 nm; G. Transverse section of a sporoblast, scale bar = 500 nm; H. Transverse section of mature spore indicating the polar tube (manubrium), peripheral ribosomes (white arrowhead) and trilaminar wall including exospore (Ex), endospore (En) and plasm membrane (black arrow), scale bar = 500 nm; I. Magnification of transverse section of manubrium showing six discontinuous concentric circles, scale bar = 100 nm.

single sac, a few were surrounded by two sacs (Fig. 3E). Notably, the thickness of the sac not even and had a maximum thickness of 730 nm at the anterior end (Fig. 3D–F). The manubrium, (homologous with a polar filament) could be observed within anterior end of spores and occupied three-quarters of spore body length (Fig. 3C). The manubrium measured 447–485 nm in diameter and exhibited six discontinuous density concentric circles (Fig. 3G, I, J) including layer 1 (unit membrane, 1.9–3.1 nm), layer 2 (electron dense, 11.8–14.3 nm), layer 3 (electron lucent, 3.7–4.9 nm), layer 4 (electron lucent, 103.1–111.8 nm), layer 5 (electron dense, 21.1–31.1 nm) and layer 6 (electron lucent, 205–236 nm). The anchoring disk was collar-like. The polaroplast was bipartite with an anterior lamellar region and a posterior tubular section (Fig. 3H). The spore wall exhibited the typical three layers, including 45–64 nm thick electron-dense exospore, 133–190 nm thick electron-lucent endospore and 8 nm thick plasma membrane (Fig. 3I).

### 3.3. Molecular analysis

The SSU rDNA sequence of two samples of the described microsporidium were 99.6% similar, with variations in only six sites along the 1415 bp fragment. A BLAST search indicated that these sequences were not identical to those of any microsporidian taxon available in GenBank, but were most similar to *Bacillidium vesiculoformis* (AJ581995, 89% over 1364 bp), isolated from the freshwater oligochaete *Nais simplex*. Other

closely related species were those isolated from a bryozoan and a *Chironomus* larva. The pairwise distances/similarities calculated by Kimura 2-parameter model among the present species and those with high sequence similarity ranged from 0.101/89.9% to 0.183/81.7% (Table 1). Maximum likelihood and Bayesian analyses of the aligned SSU rDNA produced similar topologies, although with somewhat different supported values at some branch nodes. Therefore, only the Bayesian tree is presented here, along with the bootstrap values of ML analysis. The phylogenetic analyses demonstrated that the novel *Jirovecia* species clustered with *Bacillidium* sp. and *Janacekia debaisieusi*. The *Jirovecia-Bacillidium-Janacekia* clade is a sister to the *Pseudonosema* clade. On a larger scale, bryozoan-infecting *Trichonosema* spp. arose as a basal lineage to the dichotomy of the *Jirovecia-Bacillidium-Janacekia-Pseudonosema* lineage, with representatives infecting oligochaetes and dipterans, and the *Bryonosema-Schroedera-Neperezia* clade of bryozoan and chironomid microsporidia (Fig. 4).

### 4. Taxonomic summary

#### Name: *Jirovecia sinensis* sp. n. (Microsporidia)

**Species description:** Numerous whitish xenoma-like formations in the infected host. Diplokaryotic nuclei occurred in all developmental stages. The earliest parasitic life stages observed were late meronts residing in direct contact with host cell cytoplasm. Sporoblasts were irregular in shape and matured into spores of elongated parasite cells.

**Table 1**

Comparison of similarity (above diagonal) and genetic distances (below diagonal) of *Jirovecia sinensis* sp. n. infecting the *Branchiura sowerbyi* with the most similar species and oligochaete-infecting species based on the partial 18 s rDNA.

	1	2	3	4	5	6	7	8	9	10	11
1 <i>Jirovecia sinensis</i> sp. n. MN752317		99.6	83.8	89.9	84.0	83.4	82.3	82.1	81.9	82.0	81.9
2 <i>Jirovecia sinensis</i> sp. n. MN752318	0.004		83.8	90.0	84.1	83.4	82.1	82.0	81.7	81.9	88.0
3 <i>Bacillidium</i> sp. AF104087	0.162	0.162		83.6	79.8	81.4	79.5	79.3	79.3	78.7	72.5
4 <i>Bacillidium vesiculiformis</i> AJ581995	0.101	0.100	0.164		84.5	83.2	82.0	82.1	81.8	81.7	90.6
5 <i>Trichonosema pectinatellae</i> AF484695	0.160	0.159	0.202	0.155		80.6	79.4	79.0	79.7	79.6	74.4
6 <i>Janacekia debaisieuxi</i> AJ252950	0.166	0.166	0.086	0.168	0.194		78.8	78.3	79.0	78.2	72.7
7 <i>Neoperezia chironomi</i> HQ396519	0.177	0.179	0.205	0.180	0.206	0.212		95.6	94.4	96.9	82.5
8 <i>Neoperezia semenovaiae</i> HQ396520	0.179	0.180	0.207	0.179	0.210	0.217	0.034		95.4	95.3	83.0
9 <i>Schroedera airthreyi</i> AJ749819	0.181	0.183	0.207	0.182	0.203	0.210	0.056	0.046		94.0	82.7
10 <i>Bryonosema plumatellae</i> AF484692	0.180	0.181	0.213	0.183	0.204	0.218	0.031	0.037	0.060		82.8
11 <i>Pseudonosema cristatellae</i> AF484694	0.121	0.120	0.175	0.094	0.156	0.183	0.175	0.170	0.173	0.172	

Mature spores were diplokaryotic and rod-shaped, with a tail-like posterior prolongation measuring 29.6–40.8 μm. The mature spore body measured length 17.0 ± 0.1 (14.9–18.5) μm and width 2.0 ± 0.2 (1.7–2.2) μm. Spores enclosed within the sac had a manubrium that occupied three-quarters of the spore body. The manubrium measured 447–485 nm in diameter and consisted of six discontinuous density concentric circles. Spores had a collar-shaped anchoring disk and a bipartite polaroplast, including an anterior lamellar region and a posterior section with tubules. The spore wall exhibited the typical three layers, including 45–64 nm thick electron-dense exospore, 133–190 nm thick electron-lucent endospore and 8 nm thick plasma membrane.

**Species diagnosis:** Presence of a microsporidium with characteristics described as above in the coelomocytes of oligochaete *B. sowerbyi*. Diagnosis of morphological features by light and transmission electron microscopy. Nucleic acid-based diagnosis with PCR amplification, accompanied by analysis of SSU rRNA gene sequences and comparison with the NCBI GenBank database.

**Site of infection:** coelomocytes

**Prevalence:** 11.0% (50/456)

**Type host:** *Branchiura sowerbyi* Beddard, 1892

**Type locality:** Hongze city, Jiangsu province, East China (33°21'20"N, 118°52'47"E)

**Etymology:** The species name is named after the nation of origin as it was the first *Jirovecia* species discovered in China.

**Type material:** Syntype specimens of TEM resin blocks deposited in the Museum of Hydrobiological Sciences, Institute of Hydrobiology, Chinese Academy of Sciences MTR20170520, China. The partial SSU rDNA sequence was deposited in the GenBank under accession numbers MN752317 and MN752318.

## 5. Discussion

The present work identifies and characterizes a novel species infecting the coelomocytes of *B. sowerbyi* and is the first report of aquatic oligochaete-infecting microsporidia in China. *Jirovecia sinensis* sp. n. is characterized by a diplokaryotic nucleus, rod-shaped spores and tail-like posterior prolongations, and is morphologically similar to the previously reported congeners. Six *Jirovecia* species, including *J. caudata*, *J. brevicauda*, *J. involute*, *J. lumbriculi*, *J. limnodrili* and *J. ilyodrili* were previously reported (Larsson, 1986, 1989, 1990a; Larsson and Götz, 1996). Among them, *J. lumbriculi*, *J. limnodrili* and *J. ilyodrili* easily could be distinguished from the new species by smaller spore size ( $\leq 10$  μm in spore body length). Both *J. caudata* and *J. involute* infected coelomocytes of freshwater oligochaetes, similar to *J. sinensis*. However, *J. caudata*, the type species of the genus, has a shorter tail-like posterior prolongation (10.5–17.5 vs. 29.6–40.8 μm) and does not possess a sac (Larsson, 1990a). *J. involute*, *J. brevicauda* and the new species possess a sac, however, the formation of this structure in *J. involute* and *J. sinensis* sp. n. occurred during the maturation of spores, rather than during the

sporont stage, as the case of *J. brevicauda* (Larsson, 1989; Larsson and Götz, 1996). In addition, *J. brevicauda*, the only species not infecting oligochaetes, is distinguished from *J. sinensis* by the much shorter (3.5 μm) and different origin of tail-like posterior prolongation; it is comprised of a complete constriction of the spore rather than exospore materials. Though the tail-like posterior prolongation of both *J. involuta* and *J. sinensis* is derived from mature spore exospore materials, *J. involuta* infects a different host, has a chambered and shorter tail-like posterior prolongation, and shorter polar filaments (Table 2).

Recently, the potential of microsporidian transmission through the food chain has attracted global concerns. *Inodosporus octospora* discovered from the common prawn *Palaeomon serratus* was found to be genetically identical to *Kabatana* sp. (EU682928) infecting the two-spot goby *Gobiusculus flavescens* (Stentiford et al., 2018). *G. flavescens* is omnivorous and feeds on *P. serratus*. In addition, *G. flavescens* and *P. serratus* are highly sympatric in European marine habitats. Therefore, trophic transmission for this group of parasites is highly possible. Subsequently, Sokolova and Overstreet (2018) suggested that *Apotaspula heleios* was possibly cycled between invertebrate grass shrimp and vertebrate fish through trophic transmission. Furthermore, *Jirovecia* species, discovered previously in fish intestine, was suspected to originate from the ingestion of infected oligochaetes (Lom et al., 1999). It is possible, therefore, that *Jirovecia sinensis* sp. n. could be transmitted orally to gibel carp. However, the potential for harmful effects on gibel carp by *J. sinensis* warrants further work.

More than 20 species belonging to *Jirovecia*, *Bacillidium*, *Hrabyeia*, *Mrazekia* and *Rectispora* produce rod-shaped spores (Larsson 1990a, b, 1994; Leger and Hesse, 1916; Lom and Dyková, 1990). Among them, sequence data for only several *Bacillidium* species are available, which severely limits the elucidation of their phylogenetic relationships. *Bacillidium* species were reported to be closely related to bryozoan-infecting species and *Janacekia debaisieuxi* (Morris et al. 2005). Another rod-shaped microsporidium infecting cyclopids was recently discovered, sequenced and attributed to the genus *Mrazekia* (Issi et al. 2010). Indeed, these possess features, including spore shape and the manubrium that are very similar to the species described herein. However, unlike *Jirovecia* spp., *J. debaisieuxi* is octosporogenic and sequence similarity with *J. sinensis* is low (63%). We have provided the first SSU rDNA sequence of *Jirovecia* species and demonstrated that this novel species positioned in one clade with oligochaete-infecting *Bacillidium* spp. and insect-infecting *Janacekia debaisieuxi*. Also, the polyphyly of "Mrazekiidae" was again shown, indicating that this family warrants serious revision. Taxonomically, *Jirovecia* spp. are differentiated from *Bacillidium* spp. by their typical long tail-like posterior prolongation (longer than the spore body in some cases) derived from exospore material, although both possess rod-shaped spores with a manubrium-type polar filament (Larsson 1989, 1990a). Moreover, the somewhat closely related *J. debaisieuxi* forms oval, uninucleate spores and produces sporogonial plasmodia, different from the rest of the *Jirovecia-Bacillidium-Janacekia* clade, suggesting that the current

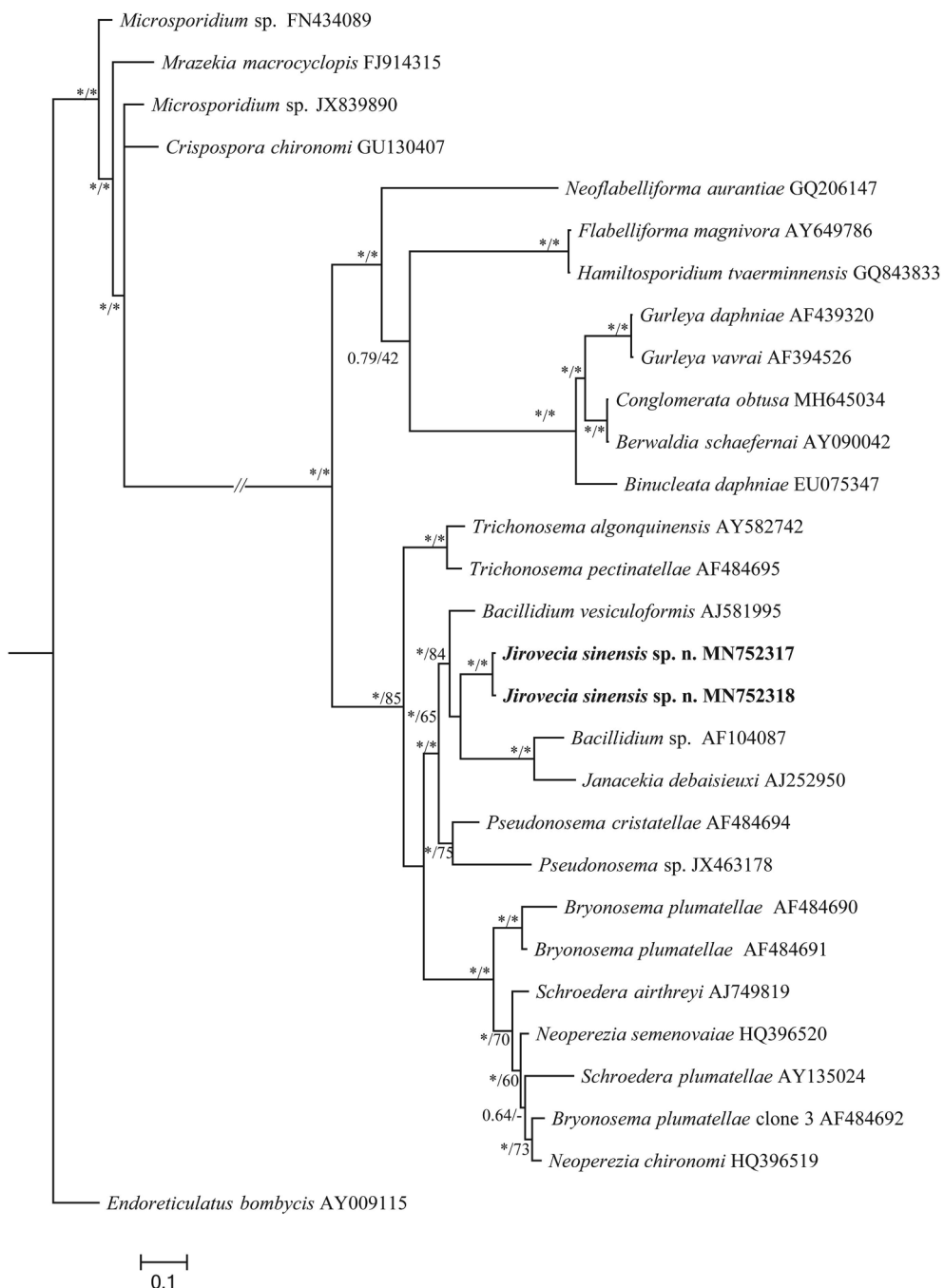


**Fig. 4.** Phylogenetic analysis of *Jirovecia sinensis* sp. n. and the aligned microsporidian species conducted by Bayesian Inference (BI) method. *Endoreticulatus bombycis* (AY009115) was used as an outgroup. The species names are followed by GenBank accession number. BI posterior probabilities/maximum likelihood bootstrap values are indicated on the branch nodes. Asterisks indicate support values > 95% and dashes indicates values < 50%, respectively. The present species was demonstrated in bold.

**Table 2**

Morphological comparison of the *Jirovecia sinensis* sp. n. infecting *Branchiura sowerbyi* with the most similar *Jirovecia* spp. reported previously.

Species	<i>Jirovecia sinensis</i> sp. n.	<i>Jirovecia involuta</i>	<i>Jirovecia caudata</i>	<i>Jirovecia brevicauda</i>
Infection sites	coelomocytes	coelomocytes	coelomocytes	fat body
Host	<i>Branchiura sowerbyi</i>	<i>Limnmodrilus hoffmeisteri</i>	<i>Limnmodrilus hoffmeisteri</i>	<i>Chironomus riparius</i> larvae
Sac	yes	yes	no	no
Spore size (μm)	1.7–2.3 × 14.9–18.5	2.1–2.5 × 16.5–18.2	1.6–2.1 × 15.4–17.5	1.4–1.5 × 20–22
Tail length (μm)	29.6–40.8	1.4–2.1	10.5–17.5	3.5
Exospore (nm)	45–64	28–34	40–45	43–85
Endospore (nm)	133–190	83–137	58–117	unknown
Polar filament (nm)	447–485	159–194	326–404	unknown
References	Present study	Larsson (1989)	Larsson (1990a, 1990b)	Larsson and Götz (1996)

molecular phylogenetic analysis has challenged the traditional taxonomy of this group of microsporidia. More sequence data is required to disclose the nature phylogenetic relationships among them, including other *Jirovecia* species.

The ultrastructural characters of the periphery of the xenoma-like, hypertrophied, microsporidia-infected coelomocytes were crucial to understand the host-parasites relationship. The analysis of *J. sinensis* showed that mature spores were localized centrally and presporogonic stages, as well as numerous pinocytosis channels, accumulated peripherally. Pinocytosis channels observed in myxozoan parasites, such as *Henneguya rotunda* infecting the gill arch and fins of *Salminus brasiliensis* and *Henneguya eirasi* infecting gills of two *Pseudoplatystoma* spp., were suggested to transport nutrients from host to the plasmodia (Naldoni et al. 2011; Moreira et al., 2014). As such, the numerous pinocytosis channels in the periphery of *J. sinensis*-infected coelomocytes may serve to enhance nutritional activity of the giant cells.

Comprehensive taxonomic characteristics from morphological, ultrastructural and molecular analysis robustly supports that the present species is new to science. This is the first *Jirovecia* sp. to be sequenced and is named *Jirovecia sinensis* sp. n.

### Declaration of Competing Interest

The authors declare that they have no known competing financial interests or personal relationships that could have appeared to influence the work reported in this paper.

### Acknowledgements

This work was partially supported by grants from the Natural Sciences Foundation of China (31772411), Natural Science Foundation of Hubei province, Young experts of Taishan Scholars Program of Shandong Province and Initiative grant for high-level personnel recruitment in Qingdao Agricultural University awarded to JY Zhang and Startup Foundation for Advanced Scholars, Hunan Agriculture University awarded to XH Liu.

### References

- Andreadis, T.G., Thomas, M.C., Shepard, J.J., 2018. *Amblyospora khaliulini* (Microsporidia: Amblyosporidae): Investigations on its life cycle and ecology in *Aedes communis* (Diptera: Culicidae) and *Acanthocyclops vernalis* (Copepoda: Cyclopidae) with redescription of the species. *J. Invertebr. Pathol.* 151, 113–125.
- Corradi, N., Keeling, P.J., 2009. Microsporidia: a journey through radical taxonomical revisions. *Fungal. Biol. Rev.* 23, 1–8.
- Franzen, C., 2008. Microsporidia: a review of 150 years of research. *Open. Parasitol.* J. 2, 1–34.
- Guindon, S., Dufayard, J.F., Lefort, V., 2010. New algorithms and methods to estimate maximum likelihood phylogenies: assessing the performance of PhyML 3.0. *Syst. Biol.* 59, 307–321.
- Hall, T.A., 1999. BioEdit: a user-friendly biological sequence alignment editor and analysis program for Windows 95/98/NT. *Nucleic. Acids. Symp. Ser.* 41, 95–98.
- Han, B., Weiss, L.M., 2017. Microsporidia: obligate intracellular pathogens within the fungal kingdom. *Microbiol. Spectr.* 5, 1–17.
- Issi, I.V., Tokarev, Y.S., Voronin, V.N., Seliverstova, E.V., Pavlova, O.A., Dolgikh, V.V., 2010. Ultrastructure and molecular phylogeny of *Mrazekia macrocyclops* sp. n. (Microsporidia, Mrazekiidae), a microsporidian parasite of *Macrocyclops albidus* (Jur.) (Crustacea, Copepoda). *Acta Protozoologica.* 49, 75–84.
- Larsson, J.I.R., 1986. On the Taxonomy of Mrazekidae: Resurrection of the Genus *Bacillidium* Janda, 1928. *J. Protozool.* 33, 542–546.
- Larsson, J.I.R., 1989. Light and electron microscope studies on *Jirovecia involuta* sp. nov. (Microspora, Bacillidiidae), a new microsporidian parasite of oligochaetes in Sweden. *Eur. J. Protistol.* 25, 172–181.
- Larsson, J.I.R., 1990a. On the cytology of *Jirovecia caudata* (Léger and Hesse, 1916) (microspora, bacillidiidae). *Eur. J. Protistol.* 25, 321–330.
- Larsson, J.I.R., 1990b. *Rectispora reticulata* gen. et sp. nov. (Microspora, Bacillidiidae), a new microsporidian parasite of *Pomatothrix hammoniensis* (Michaelsen, 1901) (Oligochaeta, Tubificidae). *Eur. J. Protistol.* 26, 55–64.
- Larsson, J.I.R., 1994. Characteristics of the genus *Bacillidium* Janda, 1928 (microspora, mrazekiidae)-Reinvestigation of the type species *B. criodrilli* and improved diagnosis of the genus. *Eur. J. Protistol.* 30, 85–96.
- Larsson, J.I.R., Götz, P., 1996. Ultrastructural evidence for the systematic position of *Jirovecia brevicauda* (Léger et Hesse, 1916) Weiser, 1985 (Microspora, Mrazekiidae). *Eur. J. Protistol.* 1996 (32), 366–371.
- Léger, L., Hesse, E., 1916. *Mrazekia*, genre nouveau de Microsporidies a spores tubuleuses. *C. R. Soc. Biol.* 79, 345–348.
- Lom, J., Dyková, I., 1990. *Hrabyeia xerkophora* n. gen. n. sp., a new microsporidian with tailed spores from the oligochaete *Nais christinae* Kasparzak, 1973. *Eur. J. Protistol.* 25, 243–248.
- Lom, J., Dyková, I., Tonguthai, K., 1999. *Kabataia* gen. n., a new genus proposed for *Microsporidium* spp. infecting trunk muscles of fishes. *Dis. Aquat. Organ.* 38, 39–46.
- Moreira, G.S., Adriano, E.A., Silva, M.R., Ceccarelli, P.S., Maia, A.A., 2014. The morphological and molecular characterization of *Henneguya rotunda* n. sp., a parasite of the gill arch and fins of *Salminus brasiliensis* from the Mogi Guaçu River, Brazil. *Parasitol. Res.* 113, 1703–1711.
- Morris, D.J., Terry, R.S., Ferguson, K.B., Smith, J.E., Adams, A., 2005. Ultrastructural and molecular characterization of *Bacillidium vesiculosiformis* n. sp. (Microspora: Mrazekiidae) in the freshwater oligochaete *Nais simplex* (Oligochaeta: Naididae). *Parasitology* 130, 31–40.
- Naldoni, J., Arana, S., Maia, A.A.M., Silva, M.R.M.D., Carriero, M.M., Ceccarelli, P.S., Adriano, E.A., 2011. Host-parasite-environment relationship, morphology and molecular analyses of *Henneguya eirasi* n. sp. parasite of two wild *Pseudoplatystoma* spp. in Pantanal Wetland, Brazil. *Vet. Parasitol.* 177, 247–255.
- Nilsen, F., 2000. Small subunit ribosomal DNA phylogeny of microsporidia with particular reference to genera that infect fish. *J. Parasitol.* 86, 128–134.
- Posada, D., 2008. jModelTest: phylogenetic model averaging. *Mol. Biol. Evol.* 25, 1253–1256.
- Ronquist, F., Huelsenbeck, J.P., 2003. MrBayes 3: Bayesian phylogenetic inference under mixed models. *Bioinformatics* 19, 1572–1574.
- Sokolova, Y.Y., Overstreet, R.M., 2018. A new microsporidium, *Apotaspora heleios* ng. n. sp., from the Riverine grass shrimp *Palaeomonetes paludosus* (Decapoda: Caridea: Palaeomonidae). *J. Invertebr. Pathol.* 157, 125–135.
- Stentiford, G.D., Feist, S.W., Stone, D.M., 2013. Microsporidia: diverse, dynamic, and emergent pathogens in aquatic systems. *Trends Parasitol.* 29, 567–578.
- Stentiford, G.D., Ross, S., Minardi, D., Feist, S.W., Bateman, K.S., Gainey, P.A., Bass, D., 2018. Evidence for trophic transfer of *Inodosporus octospore* and *Ovipleistophora arlo* n. sp. (Microsporidia) between crustacean and fish hosts. *Parasitology* 145, 1105–1117.
- Tamura, K., Stecher, G., Peterson, D., Filipski, A., Kumar, S., 2013. MEGA6: Molecular Evolutionary Genetics Analysis version 6.0. *Mol. Biol. Evol.* 30, 2725–2729.
- Thompson, J.D., Gibson, T.J., Plewniak, F., Jeanmougin, F., Higgins, D.G., 1997. The CLUSTAL-X windows interface: flexible strategies for multiple sequence alignment aided by quality analysis tools. *Nucl. Acids Res.* 25, 4876–4882.
- Vossbrinck, C.R., Debrunner-Vossbrinck, B.A., 2005. Molecular phylogeny of the Microsporidia: ecological, ultrastructural and taxonomic considerations. *Folia Parasitol.* 52, 131–142.
- Vossbrinck, C.R., Debrunner-Vossbrinck, B.A., Weiss, L.M., 2014. Phylogeny of the Microsporidia. In: Weiss, L.M., Becnel, J.J. (Eds.), *Microsporidia: Pathogens of Opportunity*. Wiley Blackwell, Oxford, pp. 203–220.
- Vávra, J., Larsson, J.R., 2014. Structure of microsporidia. In: Weiss, L.M., Becnel, J.J. (Eds.), *Microsporidia: Pathogens of Opportunity*. Wiley Blackwell, Oxford, pp. 1–70.
- Wang, Y., Li, X.C., Fu, G., Zhao, S., Chen, Y., Wang, H., Fang, W., 2017. Morphology and phylogeny of *Ameson portunus* n. sp. (Microsporidia) infecting the swimming crab *Portunus trituberculatus* from China. *Eur. J. Protistol.* 61, 122–136.
- Xu, L.W., Liu, X.H., Zhang, J.Y., Liu, G.F., Feng, J., 2017. Outbreak of enteric microsporidiosis of hatchery-bred juvenile groupers, *Epinephelus* spp., associated with a new intranuclear microporidian in China. *J. Fish. Dis.* 40, 183–189.